AD-A053 419 SRI INTERNATIONAL MENLO PARK CA F/G 18/3
EVALUATION OF THE SHOCK BLOCK TECHNIQUE FOR GENERATING UNDERWAT--ETC(U)
OCT 77 A L FLORENCE, C M ROMANDER DNA001-77-C-0210
UNCLASSIFIED DNA-4447Z NL

1 OF 1
ADA
053419

END
DATE
FILMED
6-78
DDC

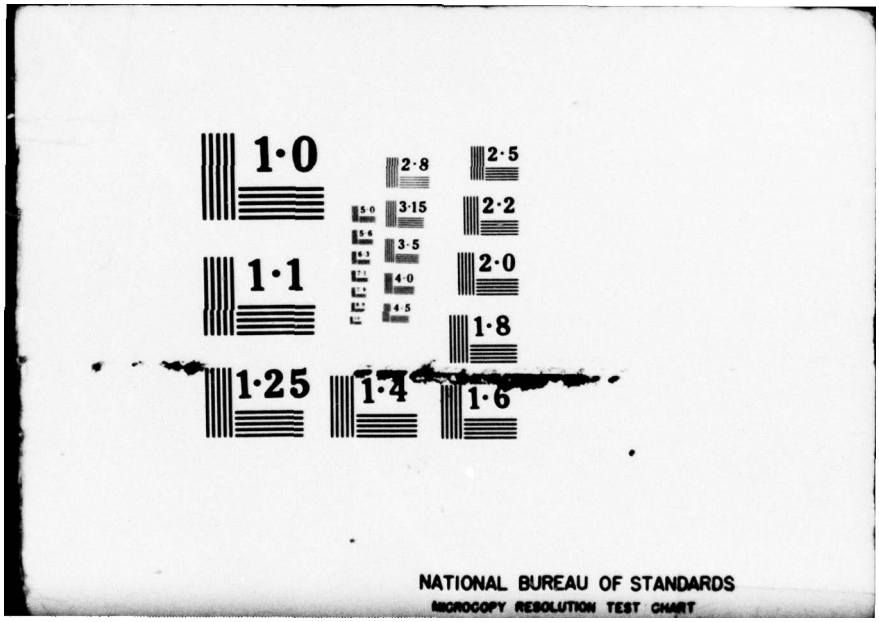
1·0
1·1
1·25
1·4
1·6
1·8
2·0
2·2
2·5
2·8
3·15
3·5
4·0
4·5
NATIONAL BUREAU OF STANDARDS
MICROCOPY RESOLUTION TEST CHART

DNA 4447Z

EVALUATION OF THE SHOCK BLOCK TECHNIQUE FOR GENERATING UNDERWATER PLANE WAVES

SRI International
333 Ravenswood Avenue
Menlo Park, California 94025

October 1977

Interim Report for Period 9 May 1977—30 September 1977

CONTRACT No. DNA 001-77-C-0210

THIS WORK SPONSORED BY THE DEFENSE NUCLEAR AGENCY
UNDER RDT&E RMSS CODE B344077464 Y99QAXSD07037 H2590D.

Prepared for
Director
DEFENSE NUCLEAR AGENCY
Washington, D. C. 20305

UNCLASSIFIED

SECURITY CLASSIFICATION OF THIS PAGE *(When Data Entered)*

REPORT DOCUMENTATION PAGE

READ INSTRUCTIONS BEFORE COMPLETING FORM

1. REPORT NUMBER	2. GOVT ACCESSION NO.	3. RECIPIENT'S CATALOG NUMBER
DNA 4447Z		

4. TITLE *(and Subtitle)*

EVALUATION OF THE SHOCK BLOCK TECHNIQUE FOR GENERATING UNDERWATER PLANE WAVES.

5. TYPE OF REPORT & PERIOD COVERED
Interim Report for Period
9 May 77—30 Sep 77

6. PERFORMING ORG. REPORT NUMBER
PYU 6383

7. AUTHOR(s)
A. L. Florence
C. M. Romander

8. CONTRACT OR GRANT NUMBER(s)
DNA 001-77-C-0210

9. PERFORMING ORGANIZATION NAME AND ADDRESS
SRI International
333 Ravenswood Avenue
Menlo Park, California 94025

10. PROGRAM ELEMENT, PROJECT, TASK AREA & WORK UNIT NUMBERS
NWED Subtask
Y99QAXSD070-37
D070

11. CONTROLLING OFFICE NAME AND ADDRESS
Director
Defense Nuclear Agency
Washington, D.C. 20305

12. REPORT DATE
October 1977

13. NUMBER OF PAGES
36

14. MONITORING AGENCY NAME & ADDRESS *(if different from Controlling Office)*
DNA, SBIE

15. SECURITY CLASS *(of this report)*
UNCLASSIFIED

15a. DECLASSIFICATION/DOWNGRADING SCHEDULE

4447Z, AD-E300 169

16. DISTRIBUTION STATEMENT *(of this Report)*

Approved for public release; distribution unlimited.

17. DISTRIBUTION STATEMENT *(of the abstract entered in Block 20, if different from Report)*

18. SUPPLEMENTARY NOTES

This work sponsored by the Defense Nuclear Agency under RDT&E RMSS Code B344077464 Y99QAXSD07037 H2590D.

19. KEY WORDS *(Continue on reverse side if necessary and identify by block number)*

Explosives
Underwater
Waves
Submarines

20. ABSTRACT *(Continue on reverse side if necessary and identify by block number)*

Underwater Explosions Research Division has developed a shock block technique for generating underwater plane waves for the Defense Nuclear Agency. The technique was designed to produce a pulse that would simulate the pulse generated by an underwater nuclear explosion and was developed to improve the current method of loading submarine sections in which the energy source is concentrated as either a large sphere or a single line of explosive. →next page

DD FORM 1 JAN 73 1473 EDITION OF 1 NOV 65 IS OBSOLETE

UNCLASSIFIED

SECURITY CLASSIFICATION OF THIS PAGE *(When Data Entered)*

410 281

JOB

20. Abstract (Continued)

SRI International has evaluated the shock block technique. This report discusses our work and recommends improvements. Examination of the experimental results revealed that the pulse generated by the equally spaced array of horizontal strands of Primacord explosive forming the shock block was of much shorter duration than predicted by superposition of the pulses from the individual strands. Instead of the required long rectangular pulse, the technique produces a short half-sine wave pulse.

We postulated that the expanding cylindrical shock wave from a single detonated strand is reflected by the similar shock waves from the neighboring strands to cause converging unstable flow of the hot gas filament. This mixing flow enhances energy extraction by transferring heat from the hot gas to the water throughout the volume of the gas filament. We conducted simple experiments with a thin strand of explosive located on the axis of a water-filled steel pipe and produced results that are consistent with the quenching postulate.

The work suggested the use of a helical coil of Primacord wrapped on a disposable cylindrical mandrel as an alternative to the straight strand of Primacord. The coil axis is horizontal and the pitch is the smallest that allows reliable detonation of the complete strand forming the helix without appreciable displacement. Simple experiments with coils in a water-filled steel tube produced rectangular pulses of durations equal to detonation times. In these simulations, high frequency pressure oscillations are superposed on the rectangular pulse; however, in an array, oscillations will be of much higher frequency so that the pulse may be smoothed out by viscous damping.

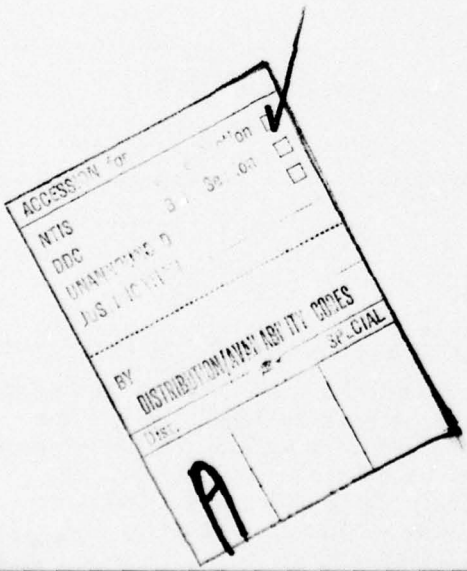

Conversion factors for U.S. customary to metric (SI) units of measurement

To Convert From	To	Multiply By
angstrom	meters (m)	1.000 000 X E -10
atmosphere (normal)	kilo pascal (kPa)	1.013 25 X E +2
bar	kilo pascal (kPa)	1.000 000 X E +2
barn	meter^2 (m^2)	1.000 000 X E -28
British thermal unit (thermochemical)	joule (J)	1.054 350 X E +3
calorie (thermochemical)	joule (J)	4.184 000
cal (thermochemical)/cm^2	mega joule/m^2 (MJ/m^2)	4.184 000 X E -2
curie	*giga becquerel (GBq)	3.700 000 X E +1
degree (angle)	radian (rad)	1.745 329 X E -2
degree Fahrenheit	degree kelvin (K)	$t_K = (t°f + 459.67)/1.8$
electron volt	joule (J)	1.602 19 X E -19
erg	joule (J)	1.000 000 X E -7
erg/second	watt (W)	1.000 000 X E -7
foot	meter (m)	3.048 000 X E -1
foot-pound-force	joule (J)	1.355 818
gallon (U.S. liquid)	meter^3 (m^3)	3.785 412 X E -3
inch	meter (m)	2.540 000 X E -2
jerk	joule (J)	1.000 000 X E +9
joule/kilogram (J/kg) (radiation dose absorbed)	Gray (Gy)	1.000 000
kilotons	terajoules	4.183
kip (1000 lbf)	newton (N)	4.448 222 X E +3
kip/inch^2 (ksi)	kilo pascal (kPa)	6.894 757 X E +3
ktap	newton-second/m^2 ($N-s/m^2$)	1.000 000 X E +2
micron	meter (m)	1.000 000 X E -6
mil	meter (m)	2.540 000 X E -5
mile (international)	meter (m)	1.609 344 X E +3
ounce	kilogram (kg)	2.834 952 X E -2
pound-force (lbs avoirdupois)	newton (N)	4.448 222
pound-force inch	newton-meter (N·m)	1.129 848 X E -1
pound-force/inch	newton/meter (N/m)	1.751 268 X E +2
pound-force/foot^2	kilo pascal (kPa)	4.788 026 X E -2
pound-force/inch^2 (psi)	kilo pascal (kPa)	6.894 757
pound-mass (lbm avoirdupois)	kilogram (kg)	4.535 924 X E -1
pound-mass-foot^2 (moment of inertia)	kilogram-meter^2 ($kg·m^2$)	4.214 011 X E -2
pound-mass/foot^3	kilogram/meter^3 (kg/m^3)	1.601 846 X E +1
rad (radiation dose absorbed)	**Gray (Gy)	1.000 000 X E -2
roentgen	coulomb/kilogram (C/kg)	2.579 760 X E -4
shake	second (s)	1.000 000 X E -8
slug	kilogram (kg)	1.459 390 X E +1
torr (mm Hg, 0° C)	kilo pascal (kPa)	1.333 22 X E -1

*The becquerel (Bq) is the SI unit of radioactivity; 1 Bq = 1 event/s.
**The Gray (Gy) is the SI unit of absorbed radiation.

CONTENTS

ILLUSTRATIONS

I SUMMARY

The Underwater Explosions Research Division (UERD)* is developing for DNA a technique for generating a plane wave in water to simulate the pulse generated by an underwater nuclear explosion. The technique is being developed to improve the current method of loading submarine sections in which the energy source is concentrated as a large sphere or as a single line of explosive.

Our objective is to assist DNA and UERD in developing this technique. This report examines the shock block version, which is a square array of equally spaced parallel line charges of Primacord, as shown in Figure 1. The examination consists of evaluating the results of UERD tests carried out with a single horizontal strand, a short vertical sheet of horizontal strands, and the small final square array of horizontal strands. The evaluation is aimed at assessing the suitability of the method for testing full-scale submarine sections. In addition to providing a plane wave, the pulse shape should have a pressure that rises rapidly to a plateau where it should remain long enough to provide the required pulse length. Our main conclusion is that the shock block generates a plane wave pulse having pressures that are large enough but a rise time that requires shortening. The most important limitation is that the pulse duration of the horizontal strands is much shorter than that of the single strand. Section III explains this pulse shortening. The mechanism that shortens the pulse appears to be inherent in the shock block configuration; the pulse duration would not be lengthened by increasing the strand lengths. Section IV suggests an alternative configuration of the Primacord array.

---

*David W. Taylor Naval Ship Research and Development Center, Portsmouth, Virginia 23709.

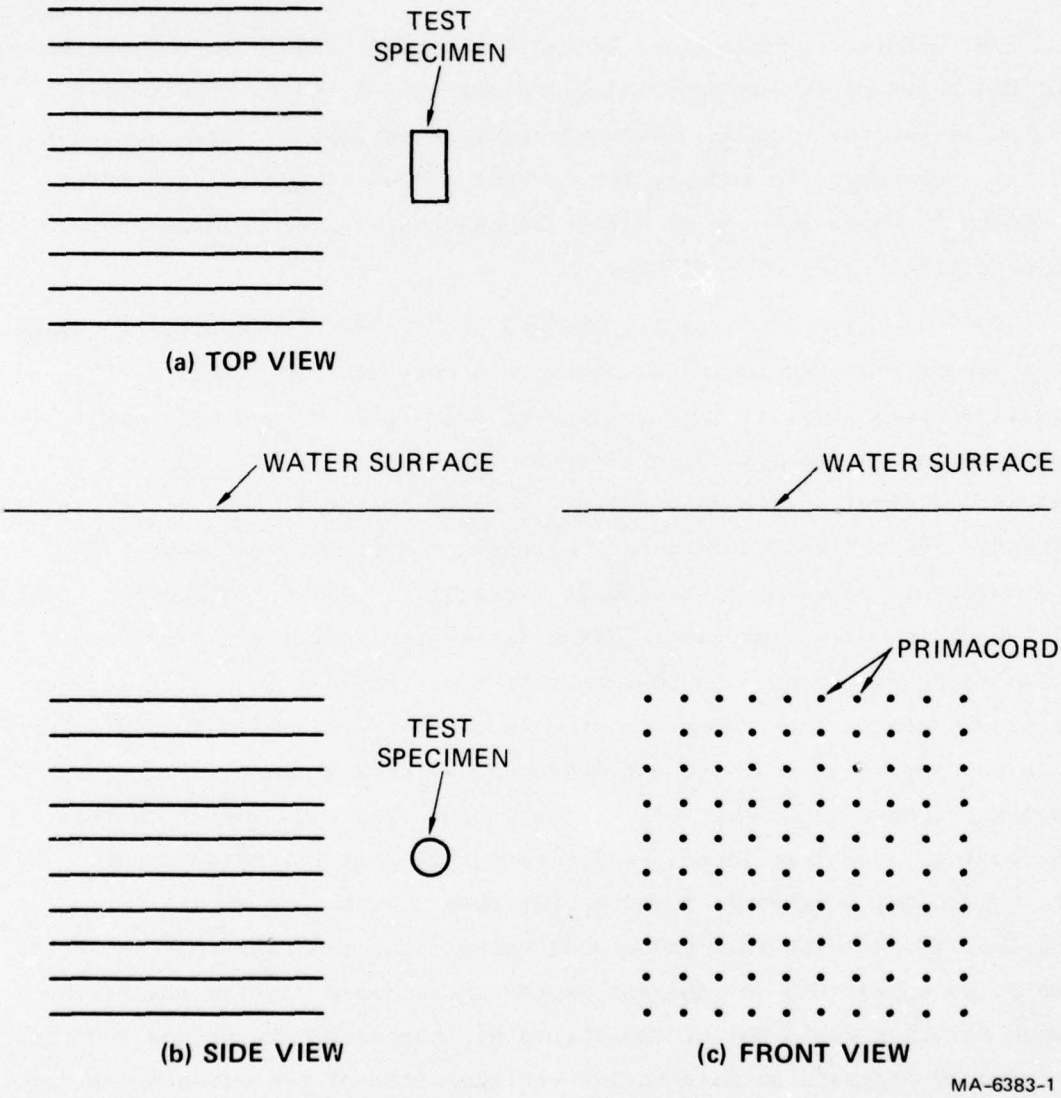

FIGURE 1 SHOCK BLOCK CONFIGURATION

II EXAMINATION OF THE UERD TEST RESULTS

Our approach to the examination of the UERD test results was to superpose the pressure pulses obtained from the single strand test in an attempt to reproduce the pulses of the sheet and block tests.

Figures 2, 3, and 4 show the configurations for the single strand, the sheet, and the block tests along with the pressure transducer locations. The pressure pulses recorded at location 4 for the line, sheet, and block sources are shown in Figures 5, 6, and 7. The corresponding pulse durations are approximately 3.2, 1.6, and 0.9 msec so that the durations of the sheet and block pulses are considerably shorter than the duration of the line pulse.

Each pulse in the line test was represented by the formula

$$P(r,t) = P_n(r)e^{-\alpha_n(t_n-t)} \qquad t > t_n \qquad (1)$$

to facilitate the pressure superposition process, where P_n is the initial peak pressure, t_n is the arrival time, and α_n is a decay parameter. The subscript n gives the location number shown in Figure 2 (n = 1-5, 7-9, 11, 12). The values of α_n and P_n were determined for each location by equating the pressure P in formula (1) to the pressure recorded at times $t_n - t$ = 0.25 and 1.25 msec. Table 1 lists the resulting values of α_n and P_n. The pulse is insensitive to the angle θ between the strand axis and a ray from the end next to the pressure transducers; in Test 8830, the angular range was $0 \le \theta \le 45°$. Thus, dependence on θ was omitted from formula (1). The peak pressure was represented by

$$P_n = \left(\frac{r_2}{r_n}\right)^{\lambda_n} P_2$$

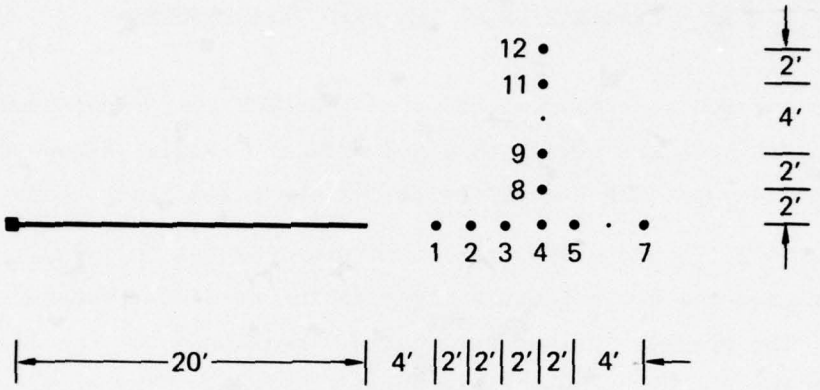

(a) TOP VIEW

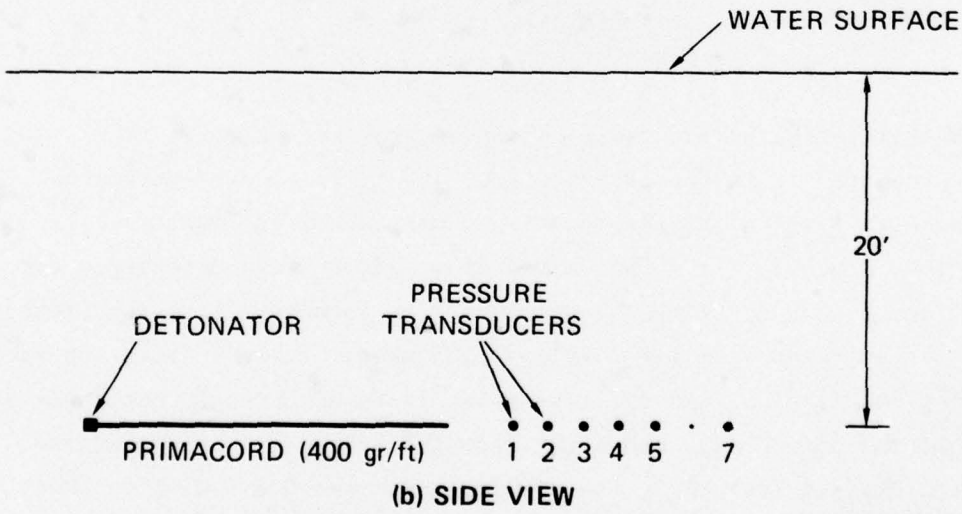

(b) SIDE VIEW

MA-6383-2

FIGURE 2 CONFIGURATION OF UERD TEST 8830 FOR PRESSURES FROM A SINGLE STRAND OF PRIMACORD

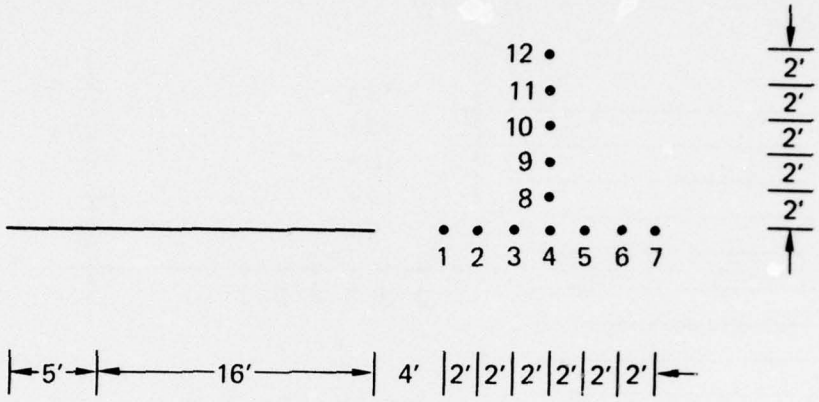

(a) TOP VIEW

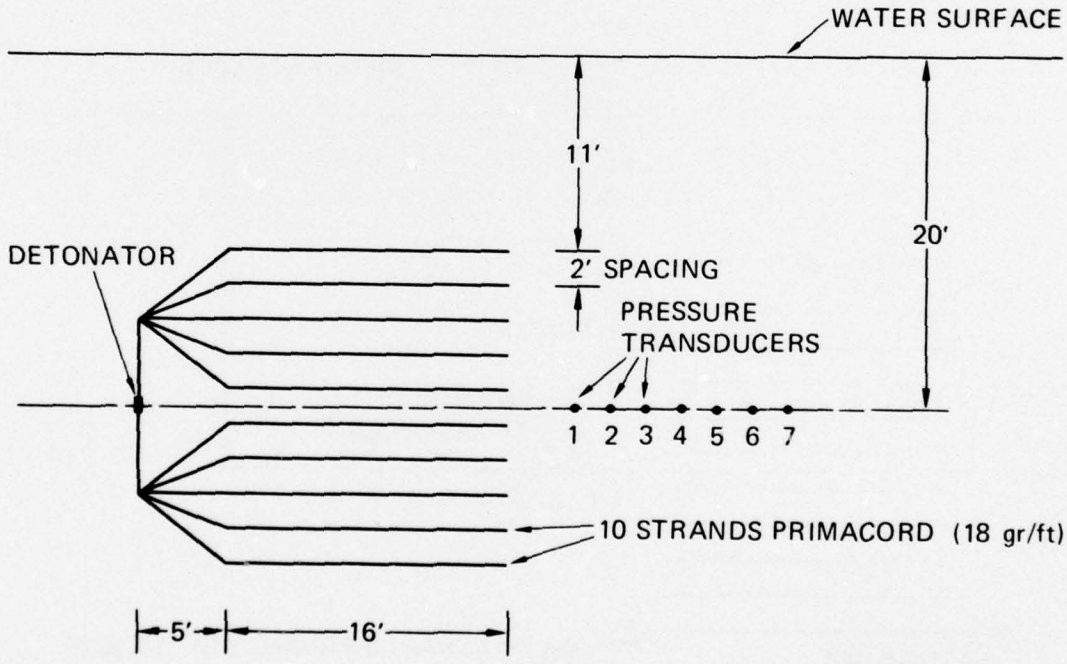

(b) SIDE VIEW

MA-6383-3

FIGURE 3 CONFIGURATION OF UERD TEST 8838 FOR PRESSURES FROM A SHEET OF 10 STRANDS OF PRIMACORD

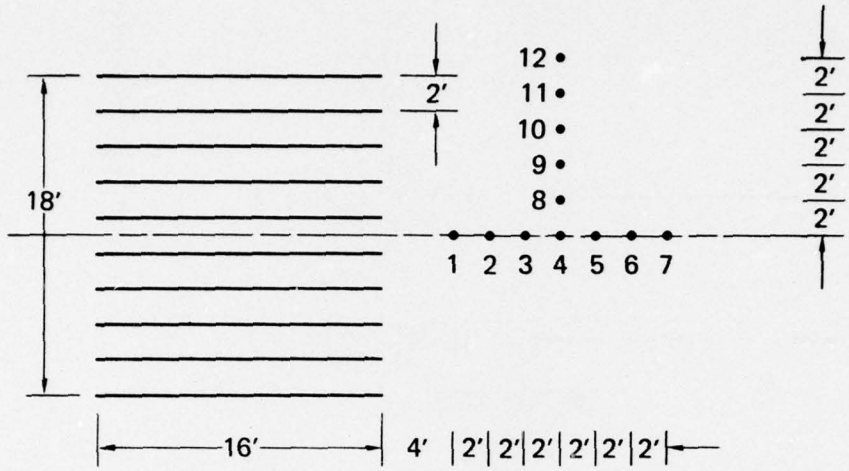

(a) TOP VIEW

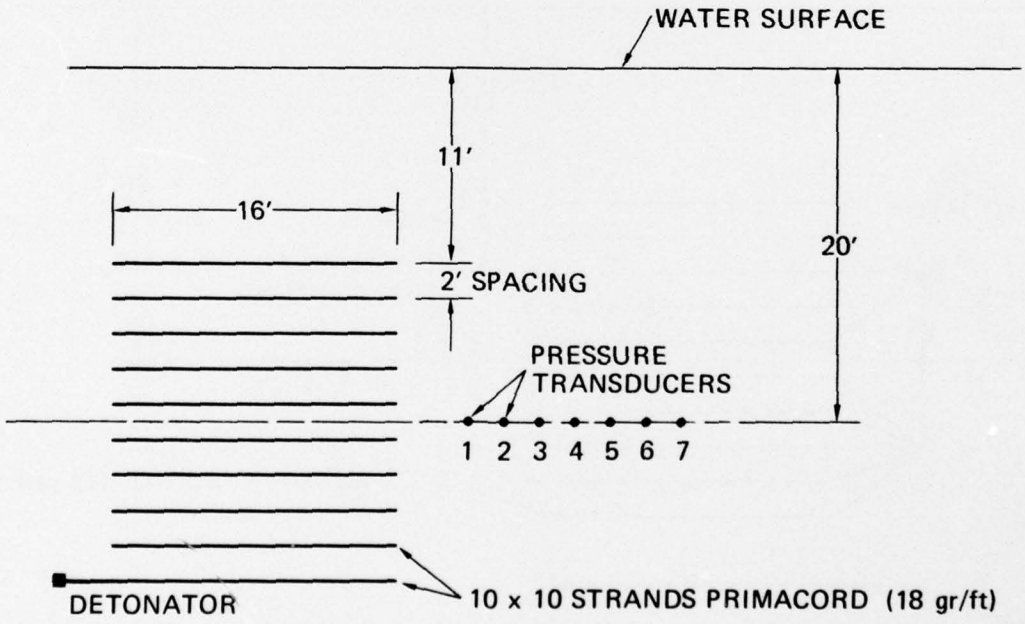

(b) SIDE VIEW

MA-6383-4

FIGURE 4 CONFIGURATION OF UERD TEST 8842 FOR PRESSURES FROM A BLOCK OF 100 STRANDS OF PRIMACORD

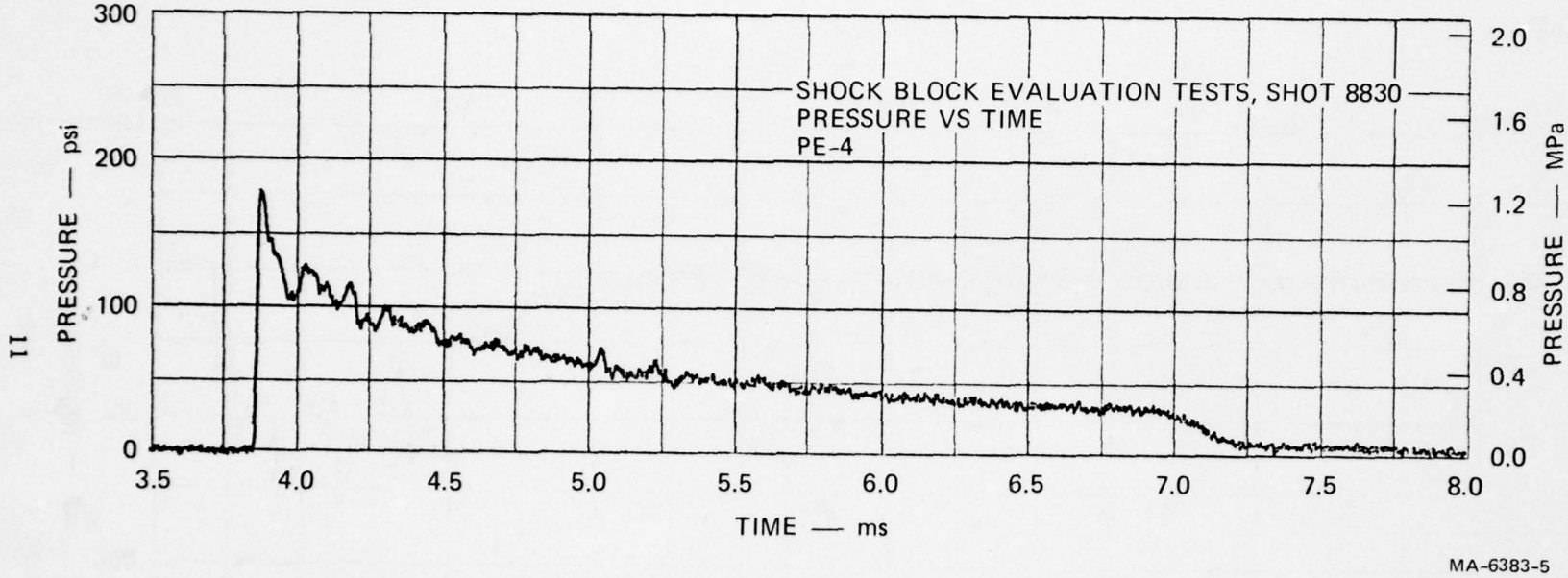

FIGURE 5 PRESSURE PULSE AT LOCATION 4 FROM SINGLE PRIMACORD STRAND

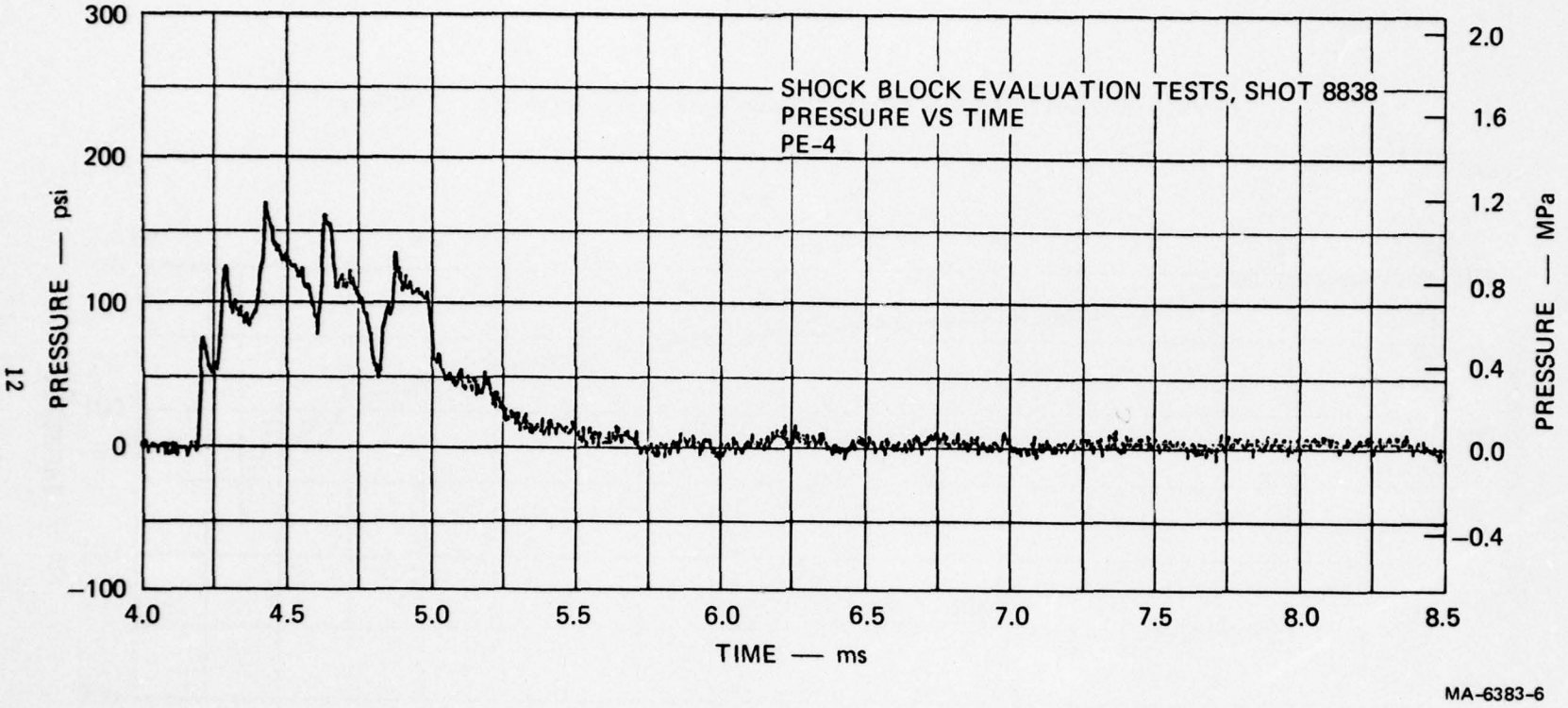

FIGURE 6 PRESSURE PULSE AT LOCATION 4 FROM SHEET OF 10 PRIMACORD STRANDS

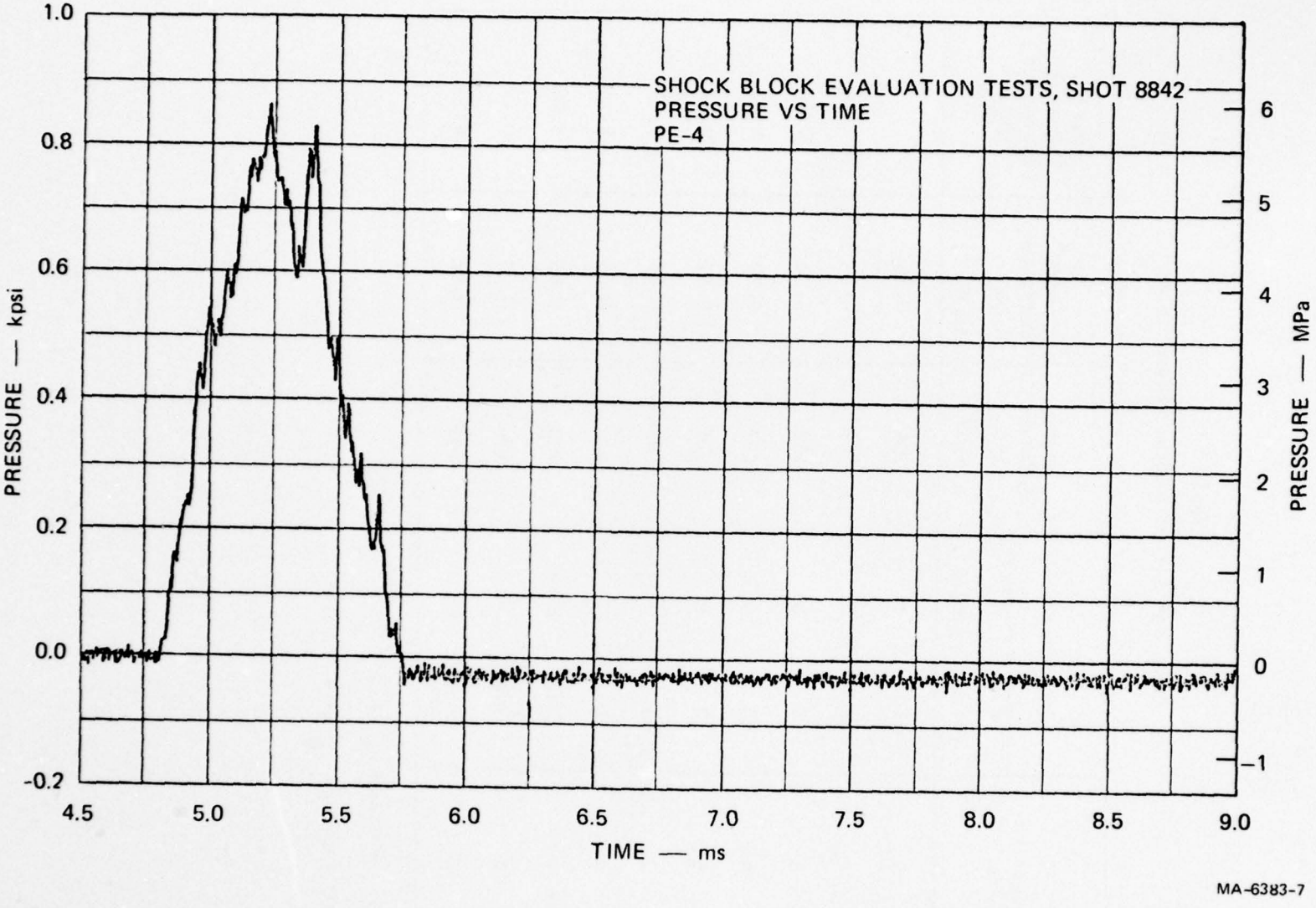

FIGURE 7 PRESSURE PULSE AT LOCATION 4 FROM BLOCK OF 100 PRIMACORD STRANDS

Table 1

Data for Fit of Single Strand Pulse

Location n	Coordinate		Peak Pressure P_n (psi)	Decay[a] Parameter α_n ($msec^{-1}$)	Peak[b] Pressure Parameter λ_n
	r (ft.)	θ (deg.)			
1	4	0	268	0.96	--
2	6	0	184	0.66	--
3	8	0	156	0.70	0.58
4	10	0	135	0.70	0.60
5	12	0	118	0.67	0.64
7	16	0	93	0.60	0.70
8	10.2	11	135	0.65	0.58
9	10.8	22	130	0.68	0.60
11	12.8	39	134	0.79	0.42
12	14.1	45	119	0.69	0.51

a. Average α_n is $\alpha = 0.68$

b. Average λ_n is $\lambda = 0.58$

which ensures agreement at location 2. The values of λ_n required to match the pressures P_n are listed in Table 1.

Apart from the location 1 values, α_n and λ_n do not vary greatly, so it is reasonable to use the average values of α and λ. Thus the pulse for a single strand is represented by

$$P = P_2 \left(\frac{r_2}{r} \right)^{\lambda} e^{-\alpha(t_n - t)} \qquad t > t_n \qquad (2)$$

where, for the 400 grains/foot Primacord in Test 8830,

$P_2 = 184$ psi

$r_2 = 6$ ft

$\lambda = 0.58$

$\alpha = 0.68$ msec^{-1}

In formula (2), t_n is the time of arrival of the pulse. Figure 8 shows the peak pressures obtained from a fit of each experimental pulse (the recorded values are slightly higher) for comparison with peak pressures ($t = t_n$) predicted by formula (2).

The pulse of Figure 9 for location 4 was obtained by using formula (2) to superpose the pressure pulses from the 10 strands forming the sheet source in Test 8838, as shown in Figure 3. Also shown in Figure 9 is a simplified version of the experimental pulse of Figure 6 recorded at location 4 in the sheet test. Because the single strand test was carried out with Primacord having an explosive weight of 400 grains/foot, whereas the sheet strands contained 18 grains/foot, the simplified sheet pulse was amplified to provide the same initial peak pressure (multiplication factor of 3.4). The curves in Figure 9 show that the pulse from the sheet experiment terminates much earlier than the pulse obtained by assuming the validity of superposition.

Formula (1) was used also to obtain the pulse at location 4 from the shock block of Figure 4. The resulting pulse and the smoothed pulse at location 4 from Test 8842 are plotted in Figure 10. Again, the

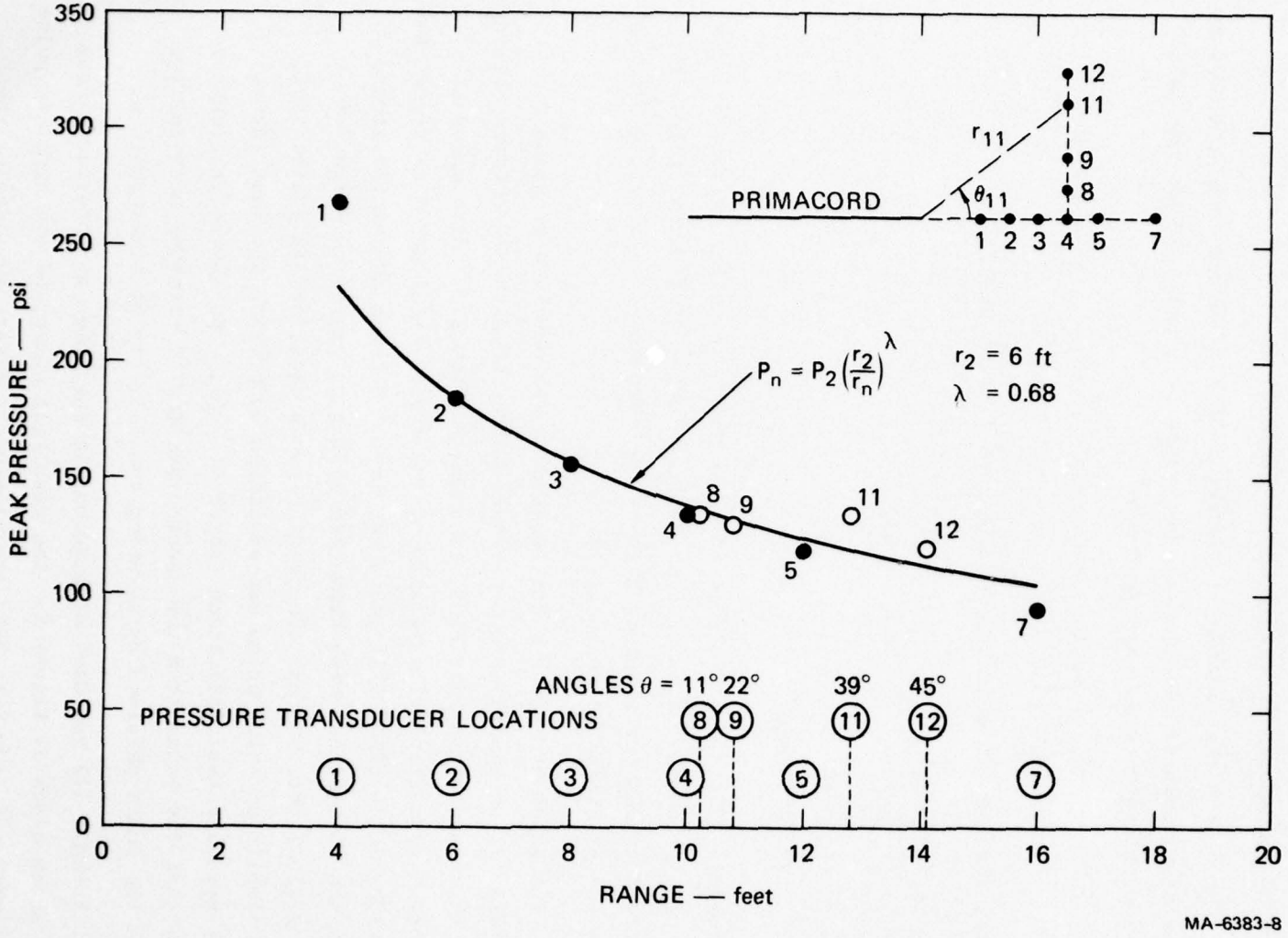

FIGURE 8 POWER LAW FIT OF EXPERIMENTAL PEAK PRESSURES

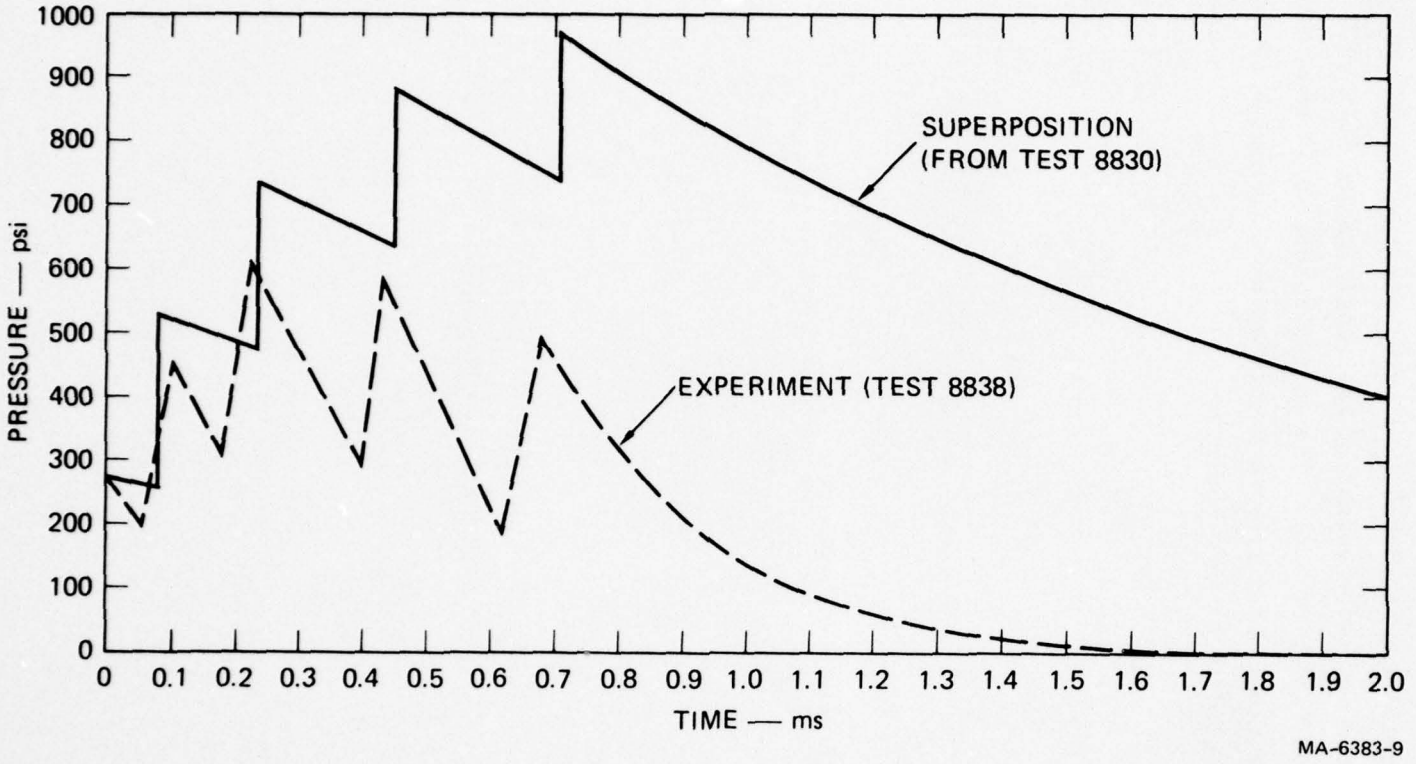

FIGURE 9 PRESSURE PULSES AT LOCATION 4 FROM SHEET AND SUPERPOSED STRANDS

experimental pulse was increased to provide the same initial peak pressure to allow for the explosive weight of the single strand being 400 grains/foot (multiplication factor of 3.4). The curves in Figure 10 show that the pulse from the block terminates much earlier than the pulse obtained by assuming the validity of superposition.

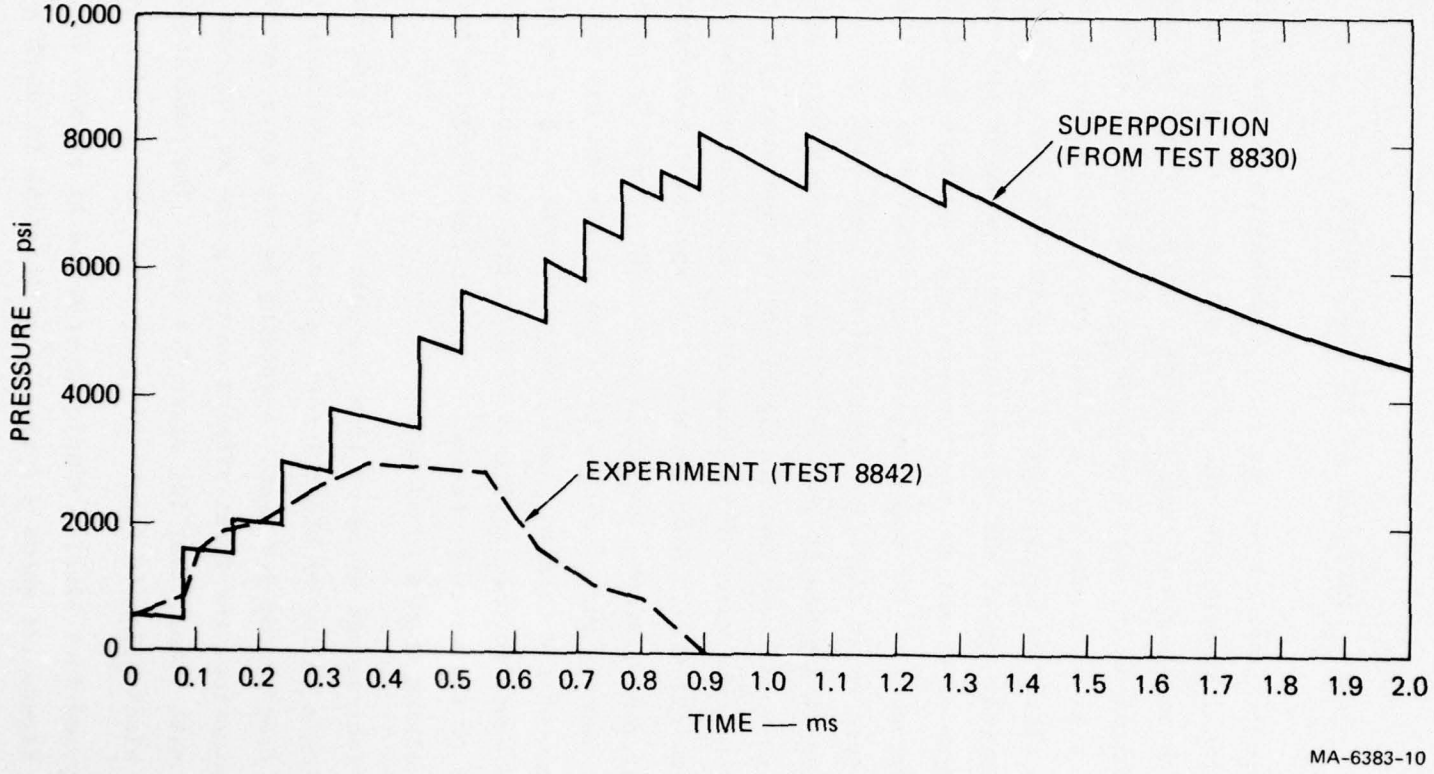

FIGURE 10 PRESSURE PULSES AT LOCATION 4 FROM BLOCK AND SUPERPOSED STRANDS

III LIMITATION OF THE SHOCK BLOCK

A possible explanation for the early termination of the shock block pulse may be found by examining the radial motion of the gas and fluid associated with an elemental length of one strand. If all strands are detonated simultaneously, then each internal strand may be envisaged as occupying the axis of a tube with a square cross section having rigid walls (Figure 11). The square tube is replaced by a circular tube to assist description. After the detonation front has swept past the elemental length of strand and has formed a high pressure gas filament, the radial component of the compressional wave travels to the rigid tube wall and reflects as an amplified compressional wave back to the gas filament. When it arrives at the cylindrical gas-water interface, the gas pressure is much lower than initially and an expansion wave propagates out to the tube where it reflects as an amplified expansion wave back to the gas filament. From the time when the first compression wave arrives at the gas filament, the fluid is set into radially convergent flow that is unstable and conducive to mixing of the hot gas and cold water. Because of the filament shape, every element of gas is subjected to mixing and hence to the rapid loss of potential mechanical work by heat transfer to the water particles. A square tube would be even more conducive to mixing than a round one.

For a 2-foot-square array of line charges, the rigid tube may be taken as having a radius of about 1 foot, giving an approximate transit time at 5000 feet/sec of 0.2 msec. According to the above description of pulse termination, the first effects on the pulse at location 4 occur after two transit times, that is, after 0.4 msec. The smoothed version of the shock block pulse in Figure 10 agrees with this prediction.

We performed four similar simple experiments to examine the quenching hypothesis. Figure 12a shows a typical configuration in which a $4\frac{1}{2}$-foot

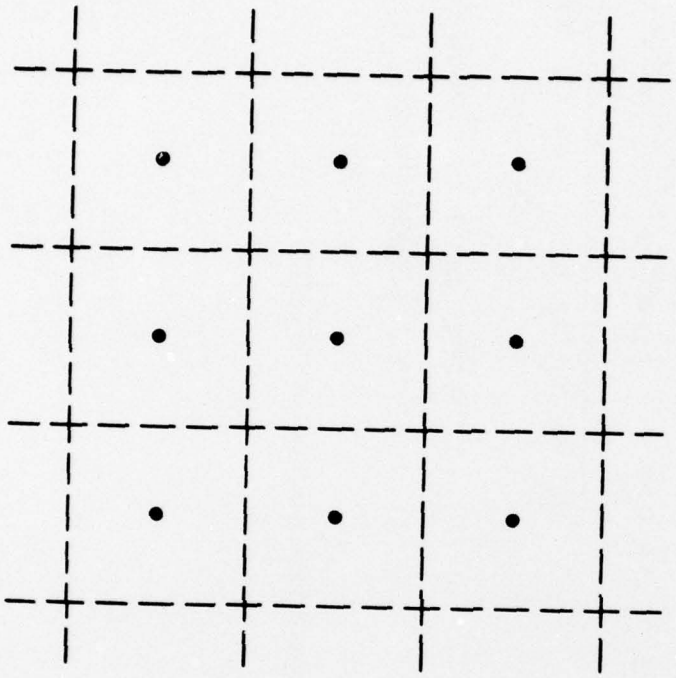

(a) PORTION OF SHOCK BLOCK

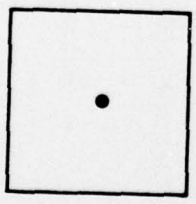

(b) STRAND IN A SQUARE TUBE

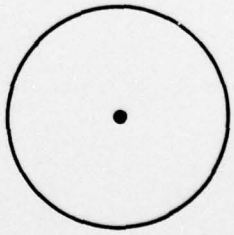

(c) STRAND IN A CIRCULAR TUBE

MA-6383-15

FIGURE 11 ARRAY REPRESENTED BY A STRAND IN A TUBE

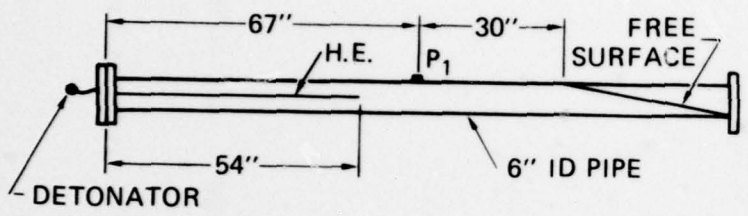

(a) LINE CHARGE CONFIGURATION

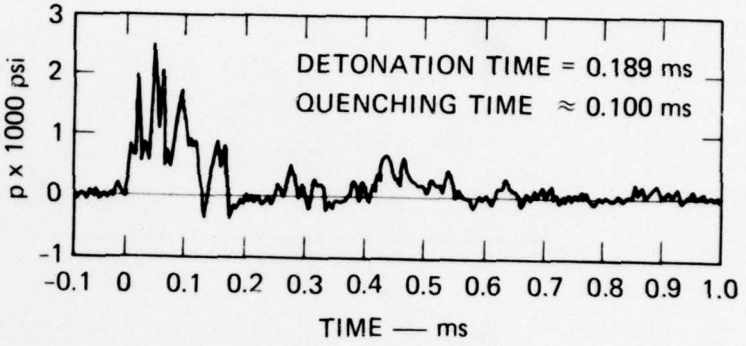

TEST 1 4.5 FT LINE CHARGE

(b) PRESSURE PULSE AT P_1

MA-6383-11

FIGURE 12 LINEAR EXPLOSIVE STRAND QUENCHING TEST

length of 35 x 35 mil Detasheet strand (about 3 grains/foot) was located on the axis of a 6-inch-diameter steel tube full of water. A pressure transducer was located in the wall of the tube 13 inches beyond the end of the strand opposite the detonated end. Figure 12b shows the resulting pressure pulse. The pulse duration is 0.18 msec, whereas superposition predicts 0.71 msec. At a cross section of the strand away from the end, quenching starts 0.1 msec after detonation at the section. Hence, the results are consistent with the quenching hypothesis.

IV ALTERNATIVE SOURCE CONFIGURATIONS

Four requirements guided the search for an alternative source configuration:

(1) Creation of gas volume at a constant rate to produce a step pulse.

(2) A long detonation time to aid generation of a long pulse.

(3) Minimization of the energy loss caused by the mixing of hot gas and cold water.

(4) A practical and economic design suitable for arrangement in an array under full scale conditions.

The first configuration examined, shown in Figure 13a, consists of a helical strand of explosive wound on a grooved steel mandrel oriented vertically in a horizontal steel tube full of water, which, for examination of the source characteristics, replaces the rest of the array. Figure 13b shows the resulting pulse measured 30 inches from the center of the 1.5-inch-diameter explosive helix. The effective pulse duration equals the detonation time. For part of the duration, the pulse is flat-topped indicating an attempt to satisfy Requirement 1. The saw-toothed rise to the plateau is attributed to progressive detonation across the pipe cross section. This observation led to the change of orientation shown in Figure 14a.

Figure 14a shows the configuration for two tests differing only by the length of the explosive strand, Test 11 with 4 feet and Test 12 with 8 feet. Figure 14b shows the pulses obtained from the two tests. Again, the pulse durations are about equal to the detonation times. The pulse of Test 11 from the shorter strand resembles a rectangular pulse but the pulse of Test 11 from the longer strand does not. The relatively slow rise time and the decay of the pulse from the longer charge is attributed to the contribution of pressure from each turn traveling faster than the

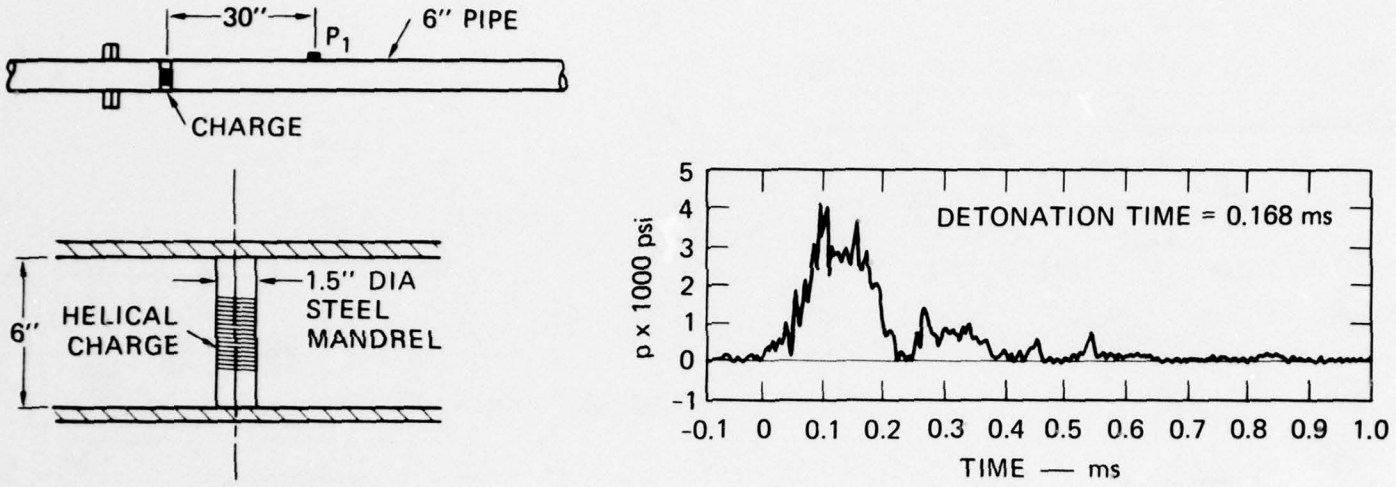

(a) CONFIGURATION OF VERTICAL HELICAL CHARGE

(b) PRESSURE PULSE AT P_1

MA-6383-12

FIGURE 13 PULSE FROM VERTICAL HELICAL STRAND OF EXPLOSIVE

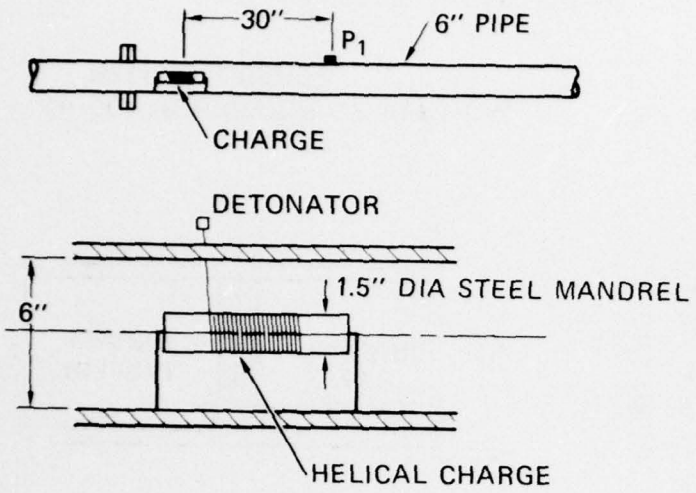

(a) CONFIGURATION OF AXIAL HELICAL CHARGE

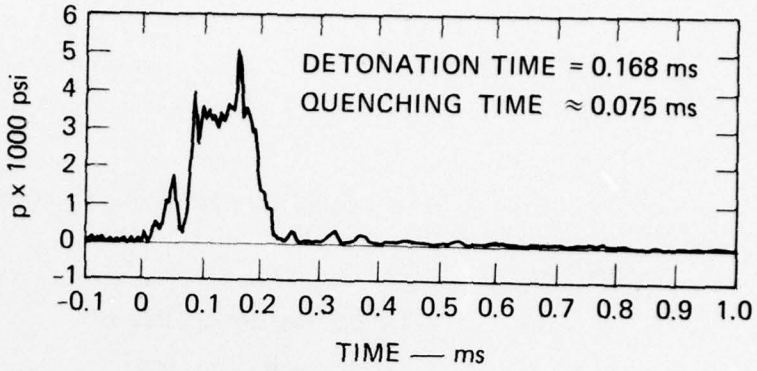

TEST 11 4 FT MDF

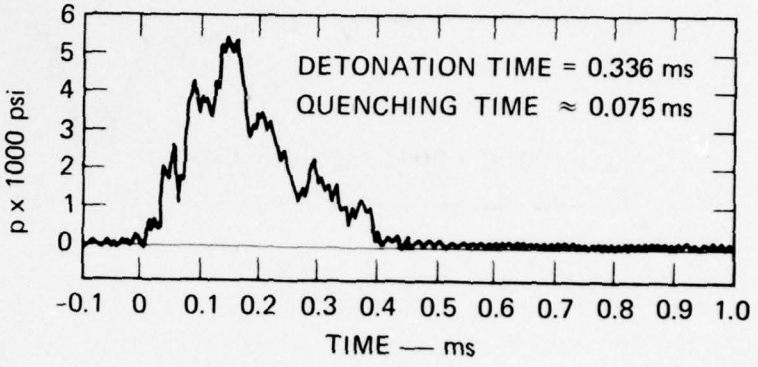

TEST 12 8 FT MDF

(b) PRESSURE PULSES AT P_1

MA-6383-13

FIGURE 14 PULSE FROM HORIZONTAL HELICAL STRAND OF EXPLOSIVE (Helix dia = 1/4 tube dia)

axial effective detonation velocity and having more time than the shorter charge to take effect. This explanation led to the configuration shown in Figure 15 where the helix has a larger diameter and occupies a central position in the tube cross section. By reducing the water area around the steel mandrel the pressure contributions from each turn are higher.

Figure 15a shows the final configuration examined in 2 tests in the steel tube. The mandrel diameter has been increased from 1½ inches to 3 inches. Figure 15b shows the pulses obtained from 12-foot and 21-foot strands. The pulse durations equal the detonation times so that Requirement 2 will be satisfied by a long coil. The shapes resemble a rectangular pulse. The undesirable feature of the pulse shape is the superposed oscillations with the highest frequency corresponding to the number of helical turns detonated per second. It is possible, however, that the oscillations would be less pronounced in an array of coils, because a steel tube cannot represent the detailed effect of the rest of the array of coils. We conjecture that the frequency content generated would be much higher and would lead to hydrodynamic damping.

Because the character of the pulse shown in Figure 15 was encouraging we decided to continue examination of the helical strand of explosive as a source. The main and practical disadvantage of the configurations is that grooved steel mandrels were used to hold the helical strand and keep it compact. We therefore decided to test the reliability of obtaining detonation of the entire coil when a simple disposable mandrel was used.

The advantage of the grooved steel mandrel is simply that the pitch of the helical strand can be kept small without the undetonated coil being blown away by the detonated coils. Thus the coil can be kept compact and gaseous regions can combine rapidly to minimize the area of the interface with water (Requirement 3). If a light disposable mandrel is used, this advantage is lost. Therefore, we conducted experiments with the general configuration shown in Figure 16 with Primacord wrapped on a Sono Tube mandrel in a water tank to test the reliability of obtaining detonation of the entire coil and to detect possible displacement of

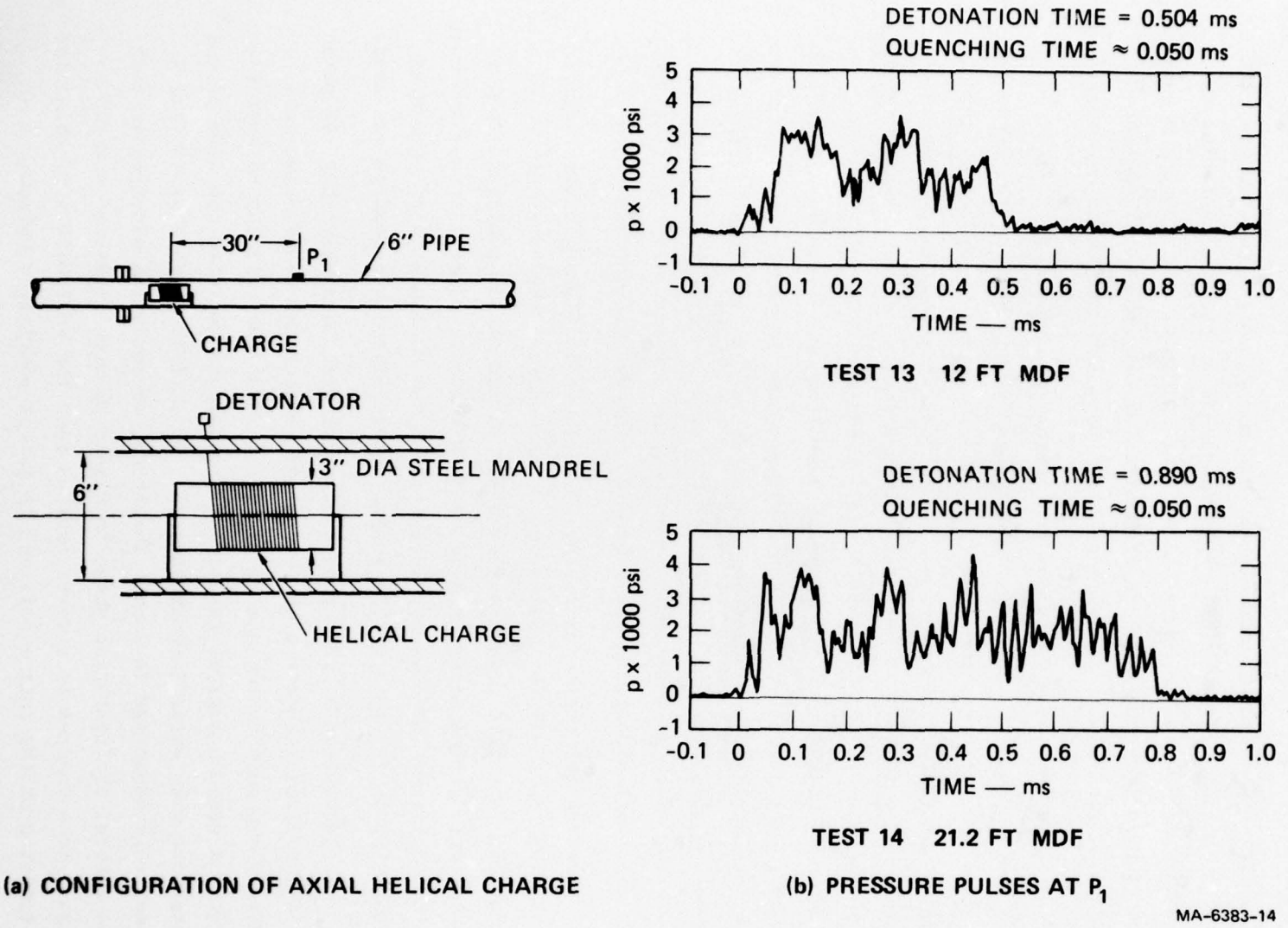

FIGURE 15 PULSE FROM HORIZONTAL HELICAL STRAND OF EXPLOSIVE (Helix dia = 1/2 tube dia)

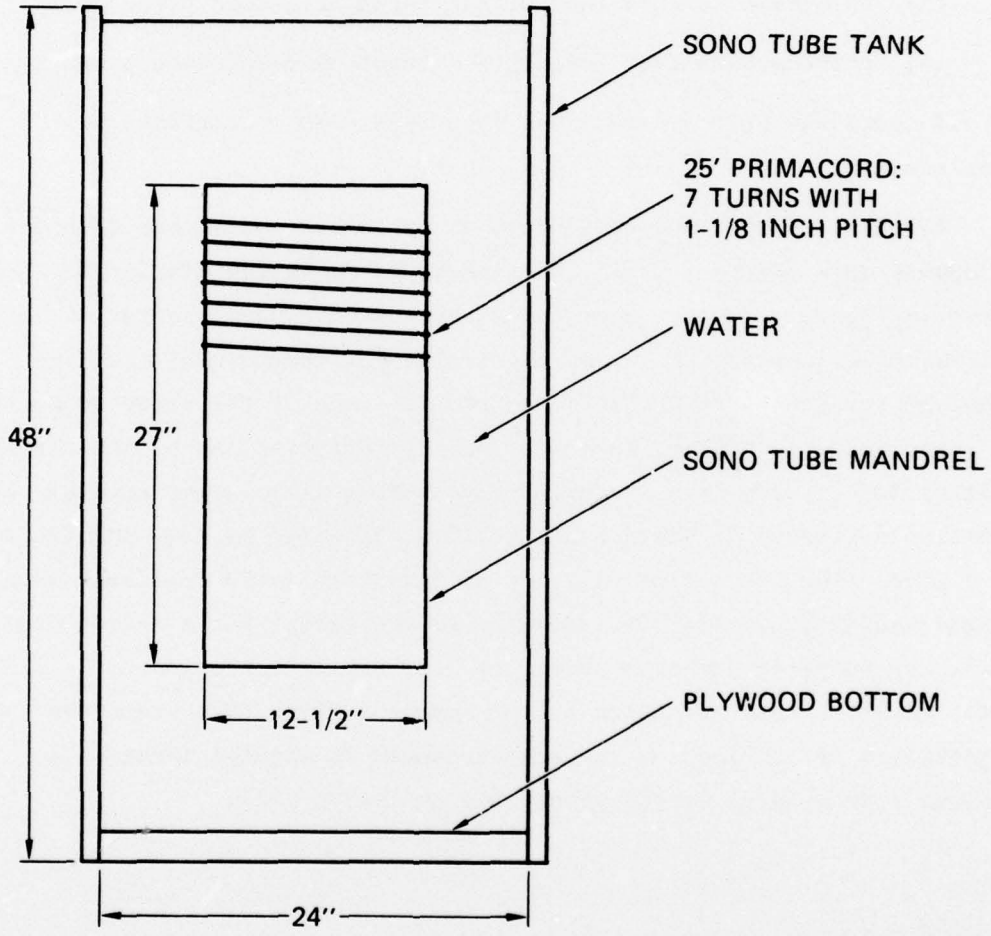

FIGURE 16 CONFIGURATION FOR RELIABILITY TESTS

coils before completion of the detonation. The Sono Tube excellently illustrates coil displacement because of the sharp cutting effect of the Primacord. Three tests were performed:

(1) Primacord 10 feet 8 inches long with 3 turns at 2-inch pitch

(2) Primacord 20 feet long with 6 turns at 4-inch pitch

(3) Primacord 25 feet long with 7 turns at 1-1/8-inch pitch.

In all cases the entire strand was detonated with negligible coil displacement.

Based on our present knowledge, we recommend continuing this development work toward a trial experiment with an array similar to that shown in Figure 1 for the shock block but using a planar array of horizontal coils in place of the straight strands. Because of the time required for pressure rarefactions from the edge of the array to be felt at a pressure transducer, each source pulse duration can be shorter than that ultimately required in full scale testing with larger arrays. At location 4 (figure 2) the measuring time unaffected by edge rarefactions is 1 msec. The detonation velocity of Primacord is 23 feet/msec so a strand length of 23 feet is adequate for the test. For a 1-foot-diameter coil, the required number of turns is 7.3, or for convenience, 8. If a pitch of 1-1/8 inch is chosen as the smallest pitch that preserves reliability of the source, the source length is about 8 inches. A 10-inch long mandrel would support the explosive coil.

DISTRIBUTION LIST

DEPARTMENT OF DEFENSE

Assistant to the Secretary of Defense
Atomic Energy
ATTN: Honorable Donald R. Cotter

Director
Defense Advanced Rsch. Proj. Agency
ATTN: Tech. Lib.
ATTN: STO, Kent Kresa
ATTN: R. Chapman
ATTN: A. Tachmindji

Defense Documentation Center
Cameron Station
12 cy ATTN: TC

Director
Defense Intelligence Agency
ATTN: DT-1C
ATTN: Tech. Lib.
ATTN: DT-2, Wpns & Sys. Div.
ATTN: DB-4C, Edward O'Farrell
ATTN: DI-7E

Director
Defense Nuclear Agency
ATTN: TISI Archives
ATTN: DDST
2 cy ATTN: SPSS
3 cy ATTN: TITL Tech. Lib

Chairman
Dept. of Defense Explo. Safety Board
ATTN: DD/S&SS

Commander
Field Command
Defense Nuclear Agency
ATTN: FCPR

Director
Interservice Nuclear Weapons School
ATTN: Doc. Con.

Director
Joint Strat. Tgt. Planning Staff, JCS
ATTN: STINFO Library

Chief
Livermore Division, Fld. Command, DNA
Lawrence Livermore Laboratory
ATTN: FCPRL

Under Sec'y of Def. for Rsch. & Engrg
ATTN: S&SS (OS)

DEPARTMENT OF THE ARMY

Dep. Chief of Staff for Rsch. Dev. & Acq.
ATTN: Tech. Lib.
ATTN: DAMA-CSM-N, LTC G. Ogden

DEPARTMENT OF THE ARMY (Continued)

Commander
Harry Diamond Laboratories
ATTN: DRXDO-TI, Tech. Lib.
ATTN: DELHD-NP

Commander
U.S. Army Armament Command
ATTN: Tech. Lib.

Director
U.S. Army Ballistic Research Labs.
ATTN: Tech. Lib. Edward Baicy

Commander
U.S. Army Communications Cmd.
ATTN: Tech. Lib.

Director
U.S. Army Engr. Waterways Exper. Sta.
ATTN: John N. Strange
ATTN: William Flathau
ATTN: Tech Lib.

Commander
U.S. Army Mat. & Mechanics Rsch. Ctr
ATTN: Richard Shea

Commander
U.S. Army Nuclear Agency
ATTN: Tech. Lib.

DEPARTMENT OF THE NAVY

Chief of Naval Material
ATTN: MAT 0323

Chief of Naval Operations
ATTN: OP 981
ATTN: OP 03EG

Chief of Naval Research
ATTN: Tech. Lib.
2 cy ATTN: Nicholas Perrone

Officer-in-Charge
Civil Engineering Laboratory
Naval Construction Battalion Center
ATTN: R. J. Odello
ATTN: Tech. Lib.

Commander
David W. Taylor Naval Ship R & D Ctr.
ATTN: Code 2740, Y. F. Wang
ATTN: Code 11
ATTN: Code L42-3, Library
ATTN: Code 1171
ATTN: Code 1731C
ATTN: Code 174, R. D. Short
ATTN: Code 19
ATTN: 1903
ATTN: 1962

DEPARTMENT OF THE NAVY (Continued)

Commander
Naval Electronic Systems Command
Naval Electronic Systems Cmd. Hqs.
ATTN: PME 117-21A

Commander
Naval Facilities Engineering Command
ATTN: Tech. Lib.

Commander
Naval Ocean Systems Center
ATTN: Tech. Lib.

Superintendent (Code 1424)
Naval Postgraduate School
ATTN: Code 2124, Tech. Rpts. Librarian

Director
Naval Research Laboratory
ATTN: Code 8442, Hanson Huang
ATTN: Code 840, J. B. Gregory
ATTN: Code 2600, Tech. Lib.
ATTN: Code 8403, Robert O. Belshem
ATTN: Code 8440, F. Rosenthal
ATTN: Code 8403A, George J. O'Hara

Commander
Naval Sea Systems Command
ATTN: Code 03511, Carl H. Pohler
ATTN: ORD-91313, Lib.

Commander
Naval Ship Engineering Center
ATTN: NSEC 6120D
ATTN: 6105C1
ATTN: NSEC 6110.01
ATTN: NSEC 6105G
ATTN: Tech. Lib.
ATTN: NSEC 6105

Commander
Naval Ship Rsch. and Development Ctr.
ATTN: Code 17, William W. Murray
ATTN: Edward W. Palmer
ATTN: Tech. Lib.

Officer-in-Charge
Naval Surface Weapons Center
ATTN: Code WA501, Navy Nuc. Prgms. Off.
ATTN: Code 243, G. Young

Commander
Naval Surface Weapons Center
ATTN: Tech. Lib.

Commanding Officer
ATTN: Code EM, Jack Kalinowski

Commander
Naval Weapons Center
ATTN: Code 533, Tech. Lib.

Commanding Officer
Naval Weapons Evaluation Facility
ATTN: Tech. Lib

DEPARTMENT OF THE NAVY (Continued)

Director
Strategic Systems Project Office
ATTN: NSP-272
ATTN: NSP-43, Tech. Lib.

DEPARTMENT OF THE AIR FORCE

AF Geophysics Laboratory, AFSC
ATTN: SUOL, Rsch. Lib.

AF Institute of Technology, AU
ATTN: Library, AFIT Bldg. 640, Area B

AF Weapons Laboratory, AFSC
ATTN: SUL

DEPARTMENT OF ENERGY

Department of Energy
Division of Headquarters Services
ATTN: Doc. Con. for Class. Tech. Lib.

University of California
ATTN: Tech. Info., Dept. L-3

Los Alamos Scientific Laboratory
ATTN: Doc. Control for Reports Lib.

Sandia Laboratories
Livermore Laboratory
ATTN: Doc. Control for Tech. Lib.

Sandia Laboratories
ATTN: Doc. Con. for 3141, Sandia Rpt. Coll.

DEPARTMENT OF DEFENSE CONTRACTORS

Agbabian Associates
ATTN: M. Agbabian

Battelle Memorial Institute
ATTN: Tech. Lib.

The BDM Corporation
ATTN: Tech. Lib.

The Boeing Company
ATTN: Aerospace Library

Cambridge Acoustical Assoc., Inc.
ATTN: M. C. Junger

Civil/Nuclear Systems Corp.
ATTN: T. A. Duffy

Columbia University
Dept. of Civil Engineering
ATTN: F. Dimaggio
ATTN: H. Bleich

General Dynamics Corp.
Electric Boat Division
ATTN: L. H. Chan

DEPARTMENT OF DEFENSE CONTRACTORS (Continued)

General Electric Company
TEMPO-Center for Advanced Studies
ATTN: DASIAC

IIT Research Institute
ATTN: Tech. Lib.

Institute for Defense Analyses
ATTN: IDA Librarian, Ruth S. Smith

Kaman AviDyne
ATTN: Tech Lib.
ATTN: G. Zartarian
ATTN: E. S. Criscione

Kaman Sciences Corporation
ATTN: Library
ATTN: T. Meagher

Lockheed Missiles and Space Co., Inc.
ATTN: Tech. Info. Ctr., D/COLL
ATTN: Tom Geers, D/52-33, Bldg. 205

University of Maryland
Dept. of Civil Engineering
ATTN: Bruce S. Berger

Merritt CASES, Inc.
ATTN: Tech. Lib.

DEPARTMENT OF DEFENSE CONTRACTORS (Continued)

Nathan M. Newmark
Consulting Engineering Services
ATTN: Nathan M. Newmark

Polytechnic Inst. of New York
ATTN: J. M. Klosner

R & D Associates
ATTN: Tech. Lib.

SRI International
ATTN: Burt R. Gasten
ATTN: George R. Abrahamson
ATTN: A. L. Florence
ATTN: C. M. Romander

Tetra Tech, Inc.
ATTN: Li-San Hwang
ATTN: Tech. Lib.

Weidlinger Assoc. Consulting Engineers
ATTN: Melvin L. Baron

Weidlinger Assoc. Consulting Engineers
ATTN: J. Isenberg